JOM, Vol. 72, No. 12, 2020
https://doi.org/10.1007/s11837-020-04398-9

Development of Conventional Paul Model for Tensile Modulus of Polymer Carbon Nanotube Nanocomposites After Percolation Threshold by Filler Network Density

YASSER ZARE [1] and KYONG YOP RHEE[2,3]

1.—Biomaterials and Tissue Engineering Research Group, Department of Interdisciplinary Technologies, Breast Cancer Research Center, Motamed Cancer Institute, ACECR, Tehran, Iran. 2.—Department of Mechanical Engineering, College of Engineering, Kyung Hee University, 1 Seocheon, Giheung, Yongin, Gyeonggi 449-701, Republic of Korea. 3.—e-mail: rheeky@khu.ac.kr

In this paper, Paul's model is advanced to forecast the tensile modulus of polymer nanocomposites reinforced by carbon nanotubes (CNT) above percolation onset. The developed model assumes the CNT network density by CNT aspect ratio (α), percolation onset and CNT density (n). The experimental results from several samples containing a filler network confirm the predictability of the advanced model. However, undesirable results are reported for the samples without the filler network. Also, both α and n directly manipulate the nanocomposite's modulus above percolation onset, because they positively influence the polymer-CNT interfacial area and network size. The reasonable effects of α, n and percolation onset on the predicted moduli of nanocomposites validate the developed Paul model.

INTRODUCTION

Carbon nanotubes (CNT) and graphene with outstanding Young's modulus,[1–3] tensile strength,[4–6] and electrical conductivity[7–12] have been used as a normal reinforcement in polymers to form nanocomposites.[13–28] However, nanoparticles like CNT form aggregates/agglomerates during the synthesis process, which reduce the surface area and disturb the networks.[29] So, the required uniform dispersion of nanoparticles in the polymer matrix is actually difficult to achieve with CNT as a reinforcing agent. Among the synthesis methods for polymer CNT nanocomposites, in situ polymerization and solution mixing have many limitations, such as being environmentally contentious, but melt blending is a fast, cost-effective, and clean technique, which has captured considerable attention in previous studies.[30,31] Some important applications of polymer CNT nanocomposites include molecular wire and electronics, high strength fibers, sensors, and field emission.[32–35]

(Received June 3, 2020; accepted September 21, 2020; published online October 19, 2020)

The networks of CNT above percolation onset cause the electrical conductivity in polymer nanocomposites.[36–38] This means that percolation onset is observed when the nanocomposite characteristics such as electrical conductivity meaningfully increase due to the nets in the polymer medium. Studies in the literature have commonly investigated the percolation threshold by measuring electrical conductivity.[39–41] Researchers have attempted to get a low percolation threshold by altering the material and processing parameters. A similar rapid change is also found in the mechanical properties of nanocomposites such as fracture toughness and stiffness.[42,43] The critical filler concentration for this abrupt increase is consistent with the electrical percolation threshold, while the mechanisms are different.

From a modeling point of view, numerous researchers have predicted the conductivity of nanocomposites by percolation onset.[44,45] Also, Ouali et al.[46] introduced the percolation term to the inverse rule of mixtures for the modulus of composites. Similarly, Lyngaae-Jorgensen et al.[47] recommended a model for the modulus of polymer blends above the percolation onset of one phase.

However, the modulus forecast in nanocomposites with percolating filler has received little attention, although it explains the unusual improvement in mechanical properties. The percolation threshold was inversely related to the particle aspect ratio in many studies.[48,49] Therefore, nanoparticle networks are created in many polymer CNT nanocomposites at low filler loadings, owing to the high aspect ratio of CNT.[50,51] Accordingly, it is rational to predict that an increase in CNT volume fraction in polymer nanocomposites may result in a sudden growth in mechanical properties.

Paul suggested a simple model for the tensile modulus of two-phase composites by matrix modulus, filler modulus, and filler volume concentration.[52] This model takes into account the macroscopically homogeneous stress in matrix and filler phases. This model was applied to predict the tensile modulus of polymer composites and nanocomposites.[53] However, this model cannot consider the networks of filler after percolation onset. In this paper, Paul's model is advanced to calculate the modulus of CNT-reinforced nanocomposites by network density. We chose the Paul model because it originated from the homogeneous stress in matrix and filler phases, which are valid in polymer CNT nanocomposites. Also, the modulus of polymer nanocomposites depends on the moduli of matrix and nanoparticles as well as filler concentrations, as properly considered by the Paul model. For these reasons, we developed the Paul model for tensile modulus of CNT-reinforced nanocomposites in this paper. The forecasts of the original and advanced models are compared using experimental data from several samples above and below the percolation threshold. Also, the reasonable impacts of the studied factors on the nanocomposite's modulus are evaluated to demonstrate the validity of the advanced Paul model.

THEORETICAL MODELS

The Paul model for tensile modulus of composites was stated[52] as:

$$E = E_{\mathrm{m}}\frac{1+(m-1)\phi_f^{2/3}}{1+(m-1)(\phi_f^{2/3}-\phi_f)} \tag{1}$$

$$m = \frac{E_{\mathrm{f}}}{E_{\mathrm{m}}} \tag{2}$$

where ϕ_f is the filler volume portion and E_{m} and E_{f} show the moduli of polymer host and filler, respectively. However, the Paul model cannot forecast the nanocomposite's modulus by filler network above percolation onset. For development of this model, the volume portion of the network after percolation onset is considered as:

$$\phi_N = (1+x)\phi_f \tag{3}$$

where x shows the network density in the samples, because the network density mainly manipulates the volume concentration of networks in nanocomposites. Actually, there is a direct relation between ϕ_N and x, because the network density directly manages the network volume fraction in nanocomposites.

Since the networked CNT significantly affects the modulus of nanocomposites, the developed Paul model expresses the relative modulus as the nanocomposite's modulus divided by the polymer matrix modulus (E/E_{m}) and by ϕ_N as:

$$E_R = \frac{1+(m-1)\phi_N^{2/3}}{1+(m-1)(\phi_N^{2/3}-\phi_N)} \tag{4}$$

The predictability of this model is assessed by the experimental modulus of reported samples above and below the percolation onset. Also, the x value is calculated by fitting the experimental data to the model.

The relative density of a 3D network is given[49] by:

$$\hat{\rho} = \frac{\rho_{\mathrm{N}}}{\rho_{\mathrm{CNT}}} = \frac{\pi N l d^2}{4L_1L_2L_3} = \frac{\pi}{4}nld^2 = \frac{\pi}{4}n\alpha d^3 \tag{5}$$

where ρ_{N} and ρ_{CNT} show the density of network and CNT, respectively. n is the total number of CNT in the periodic unit cell, d and l are the diameter and length of CNT, respectively, and $L_1L_2L_3$ is taken for simplicity. n is the CNT density and α is the aspect ratio as $\alpha = l/d$.

x in Eq. 3 can be correlated with $\hat{\rho}$ (relative density of 3D network) based on the mathematical analyses and obtained results as:

$$x = 100\hat{\rho} \tag{6}$$

which is logical, because both x and $\hat{\rho}$ are related to the network density in nanocomposites.

x is defined by net and filler properties as:

$$x = 25\pi n\alpha d^3 \tag{7}$$

Undoubtedly, if x has a positive value, this demonstrates the formation of networks in nanocomposites. However, $x < 0$ reveals the absence of networks in the samples.

In addition, the percolation onset for stiffness of CNT-reinforced nanocomposites was given[49] by:

$$\phi_p = \frac{2.2}{\alpha} \tag{8}$$

which correlates the percolation threshold with filler aspect ratio. By applying the above equation into Eq. 7, x in the developed Paul model is expressed by percolation volume fraction as:

$$x = \frac{55\pi nd^3}{\phi_p} \tag{9}$$

The impacts of net and filler properties on the modulus of nanocomposites are determined in the next section.

When the experimental moduli of samples are applied to the established model (Eq. 4), the value of x is determined. Also, α and d values are easily measured by morphological analysis. The level of n can be determined using the values of x, α and d by rearranging Eq. 7 as:

$$n = \frac{x}{25\pi\alpha d^3} \tag{10}$$

Similarly, the level of ϕ_p can be calculated by the values of x, n and d by rearrangement of Eq. 9 as:

$$\phi_p = \frac{55\pi n d^3}{x} \tag{11}$$

which shows a simple methodology for characterization of network properties by the experimental data of modulus and physical properties of nanoparticles.

RESULTS AND DISCUSSION

The original and developed models are utilized to forecast the modulus of several samples and compare the calculations with the measurements. Also, the roles of the parameters affecting the network density and modulus are estimated.

Figure 1 shows the experimental results for phenolic/single-walled carbon nanotubes (SWCNT),[54] nylon 6/multi-walled carbon nanotubes (MWCNT),[55] high density polyethylene (HDPE)/SWCNT,[56] and polypropylene (PP)/MWCNT[57] samples and the forecasts of modulus by original and advanced models. The original model commonly underestimates the modulus, due to disregarding the filler network. However, the developed model can forecast the modulus for networks above percolation onset. Hence, the developed model successfully foretells the modulus by the density of filler network. The best calculations are obtained by the x values of 2.5, 2, 0.7, and 1.3 for phenolic/SWCNT, nylon 6/MWCNT, HDPE/SWCNT, and PP/MWCNT samples, respectively, which demonstrate the relative network densities of 0.025, 0.02, 0.007, and 0.013 for these samples. As a result, the highest level of network density is shown in the phenolic/SWCNT sample, while the lowest one is reported in HDPE/SWCNT.

Obviously, a high level of network density at low filler concentration suggests a significant modulus in the polymer nanocomposite, as shown in Fig. 1a. However, a low density of CNT network, even at high volume fraction of nanofiller, makes a poor modulus, as reported for HDPE/SWCNT and PP/MWCNT samples. These outputs are due to the higher bearing capacity of a denser network. Also, it is possible to calculate the values of each parameter by the levels of other parameters, as mentioned in the previous section. For example, the value of n can be calculated when the values of x, α, and d are known. It should be noted that the developed model only considers the increased modulus as CNT concentration increases, due to the formation of bigger networks at higher CNT concentrations. In fact, the developed model cannot predict a decreased modulus as CNT concentration increases. For example, the phenolic/SWCNT sample shows a reduced modulus at CNT $>$ 0.75 wt.%; so there are no calculated results for this sample at CNT $>$ 0.75 wt.% (see Fig. 1a).

Figure 2 also clarifies the trial data and the forecasts of modulus by original and advanced models for the PP/CNT sample from Ref. 58 and poly (trimethylene terephthalate)/MWCNT from Ref. 59. The original Paul model overpredicts the modulus in these samples, but the developed model can calculate the modulus by $x < 0$, which results in a negative value for network density (see Eq. 7). The low experimental modulus shows the absence of filler network in these samples, which causes the overprediction of the Paul model. It means that the filler network was not formed in these samples and the developed model cannot predict the tensile modulus and network density for them. In other words, the developed model is capable of predicting the formation or absence of filler network in polymer CNT nanocomposites.

Generally, a high nanocomposite modulus is obtained by the formation of a filler network above the percolation threshold in the polymer matrix, which can stand the load. However, the nanoparticles below the percolation threshold do not create a network structure, demonstrating a low improved modulus. The experimental moduli fit the calculations of the advanced model at $x < 1$, showing the absence of filler net in the polymer medium. In this case, the original Paul model also overpredicts the modulus of polymer nanocomposites.

Figure 3 displays the impact of x on the relative modulus using the developed model at E_m = 2 GPa, ϕ_f = 0.02 and E_f = 1000 GPa as constant values. The best and the worst levels of modulus are observed by the highest and the lowest values of x, indicating that a high network density causes a high modulus, whereas a low density of filler network results in a low stiffness. Moreover, a high level of x causes a large modulus improvement upon increasing the filler volume fraction, which demonstrates that a high quantity of nanoparticles in the net significantly reinforces the sample.

According to Fig. 3, an x value of 2 produces a relative modulus of about 2 at ϕ_f = 0.02, whereas x = 3 gives E_R = 2.4. Also, the developed model shows the smallest relative modulus of about 1.7 with x = 1 in this condition. Therefore, the network density above percolation onset is very important, and considerably affects the nanocomposite's

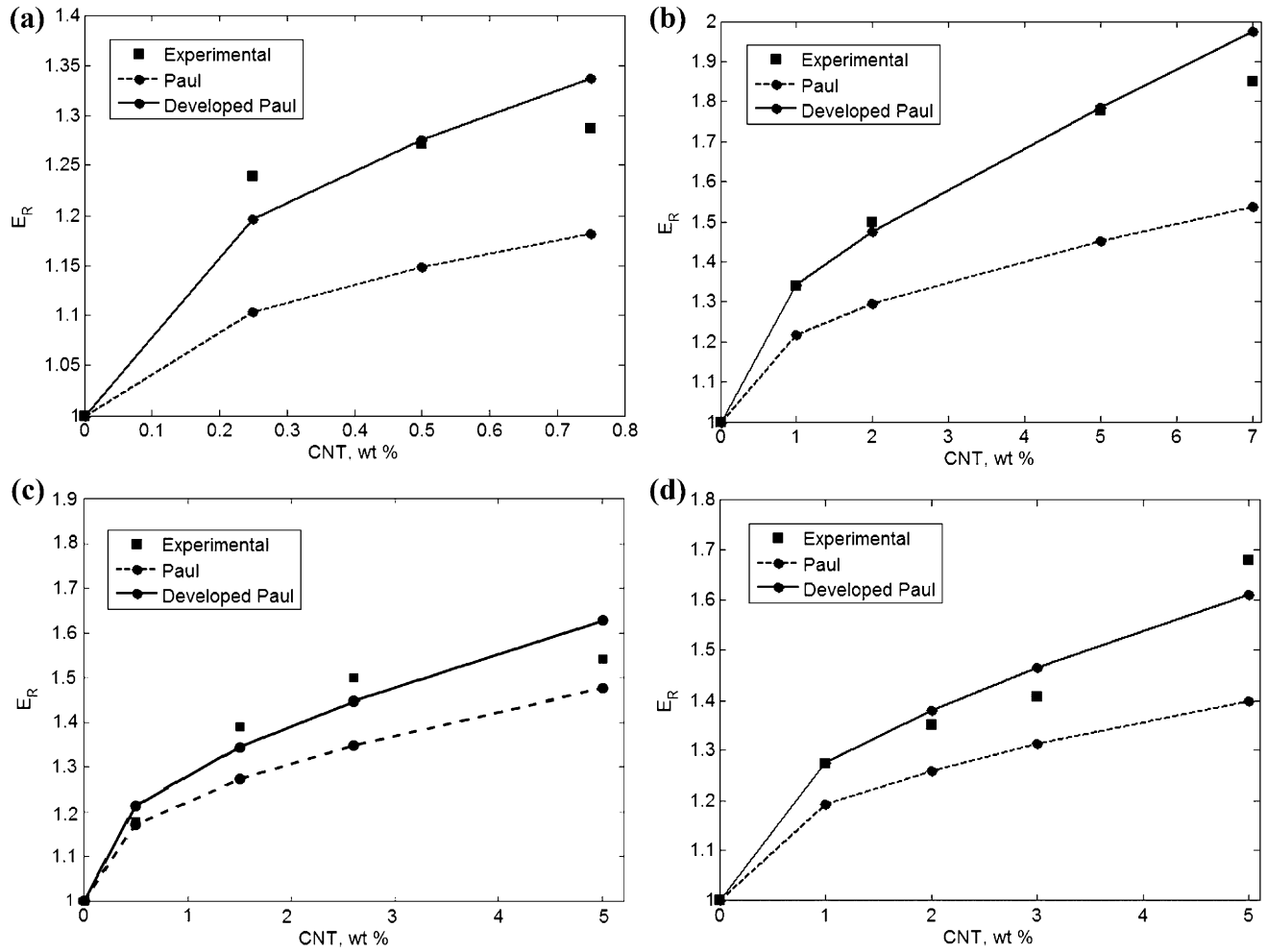

Fig. 1. The experimental results for (a) phenolic/SWCNT,[54] (b) nylon 6/MWCNT,[55] (c) HDPE/SWCNT,[56] and (d) PP/MWCNT[57] samples and the calculations of modulus by original and developed Paul models.

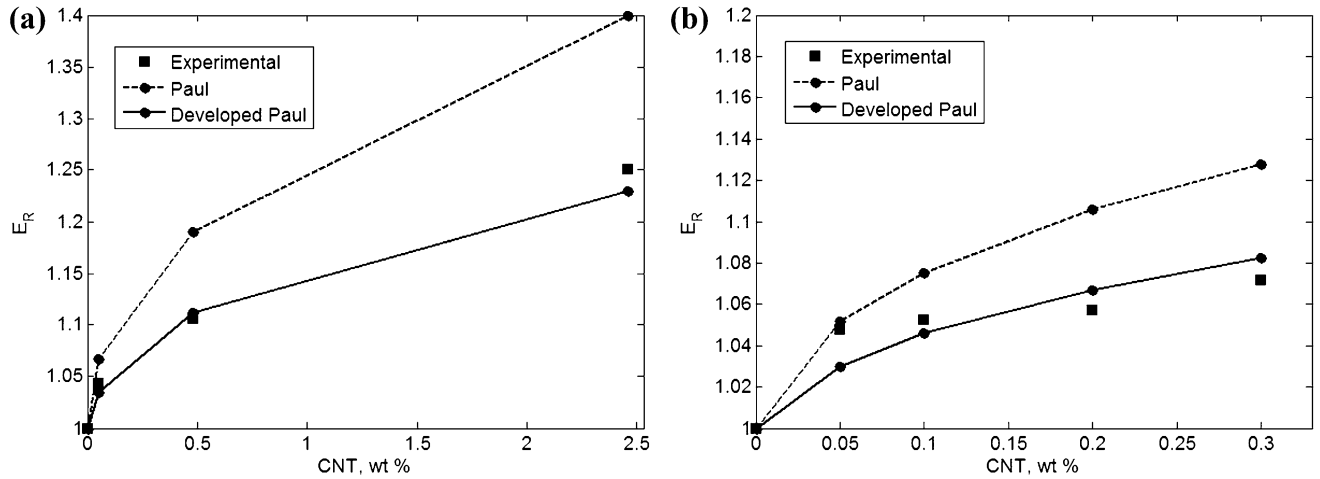

Fig. 2. The experimental data of modulus and the calculations by original and advanced Paul models for (a) PP/CNT[58] and (b) poly (trimethylene terephthalate)/MWCNT[59] samples.

modulus. The influences of different factors on the network density in polymer nanocomposites are explained in the following.

Figure 4 reveals the 3D and contour patterns for the α and n roles in the relative modulus by the advanced model at $E_m = 2$ GPa, $\phi_f = 0.02$,

d = 20 nm, and E_f = 1000 GPa. A relative modulus of 1.52 is found by α = 500 and n = 4, but the lowest level of E_R as 1.36 is reported by α = 100 and n = 0.5. As a result, both α and n directly manage the modulus of nanocomposites. α as the length per diameter of CNT determines the surface area of nanoparticles contacting the polymer matrix. A high α shows a large interfacial area between polymer medium and nanoparticles, which mainly grows the physical involvement of polymer chains by nanoparticles causing the high reinforcement.[60] Furthermore, a high α is obtained by a small diameter of nanotubes, which causes robust interfacial communications due to similar ranges of nanoparticles and polymer sizes.[61,62] Therefore, the direct correlation between the modulus of nanocomposites and α is justified according to the developed model. Previous studies also confirmed the direct influence of α on the modulus of polymer nanocomposites.[63,64] Furthermore, a high level of n as CNT density undoubtedly improves the modulus, since CNT with a high modulus and strength acts to reinforce the material. On the other hand, a low n causes a low network density, which certainly decreases the stiffness of nanocomposites. Finally, the direct impacts of both α and n parameters on the nanocomposite's modulus are correct, confirming the advanced model.

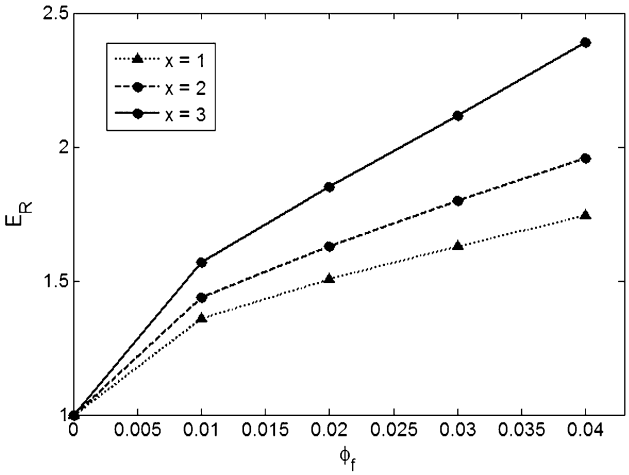

Fig. 3. The role of x level in the prediction of modulus by the developed model at E_m = 2 GPa, ϕ_f = 0.02, and E_f = 1000 GPa.

Figure 5 also presents the relative modulus depending on ϕ_p and d factors at E_m = 2 GPa, ϕ_f = 0.02, n = 1, and E_f = 1000 GPa. E_R = 1.4 is shown in d < 15 nm, while an E_R level of 2.5 is obtained by ϕ_p = 0.001 and d = 40 nm. Hence, a low modulus is only observed at slight d values, but high d and low ϕ_p produce good reinforcement. ϕ_p inversely affects the modulus of polymer CNT nanocomposites, because ϕ_p determines the minimum filler concentration, which produces the filler network. In the case of low ϕ_p, the network of nanoparticles is obtained by a low filler content, which considerably improves the modulus. However, a high ϕ_p shows the production of filler network at high ϕ_f; so the modulus of nanocomposites shows a poor range at low filler loading below the percolation onset, owing to the nonappearance of nets. Also, a low ϕ_p results in a high density of filler network, which results in a great modulus. As a result, the effect of ϕ_p on the modulus of the samples by the advanced model is as expected.

The diameter of CNT is a main parameter influencing the relative modulus according to Fig. 5. As mentioned, a low diameter of CNT is enough to see a poor modulus in nanocomposites. A low CNT diameter causes a low level of network density based on Eq. 9, while thick CNT produces a dense network. Since the stiffness of nanocomposites significantly depends on the network density, the effect of CNT diameter on the relative modulus is reasonable. Therefore, the dependence of the relative modulus on ϕ_p and d parameters is as expected, which proves the advanced model for tensile modulus of nanocomposites.

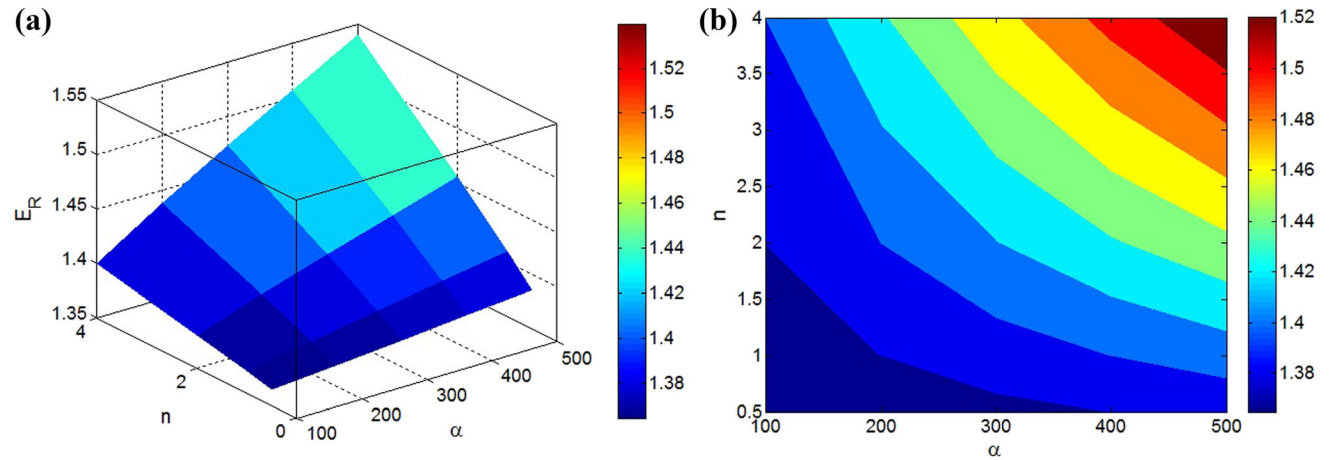

Fig. 4. The effects of α and n as network properties on the predicted relative modulus by developed model at E_m = 2 GPa, ϕ_f = 0.02, d = 20 nm, and E_f = 1000 GPa: (a) 3D and (b) contour plots.

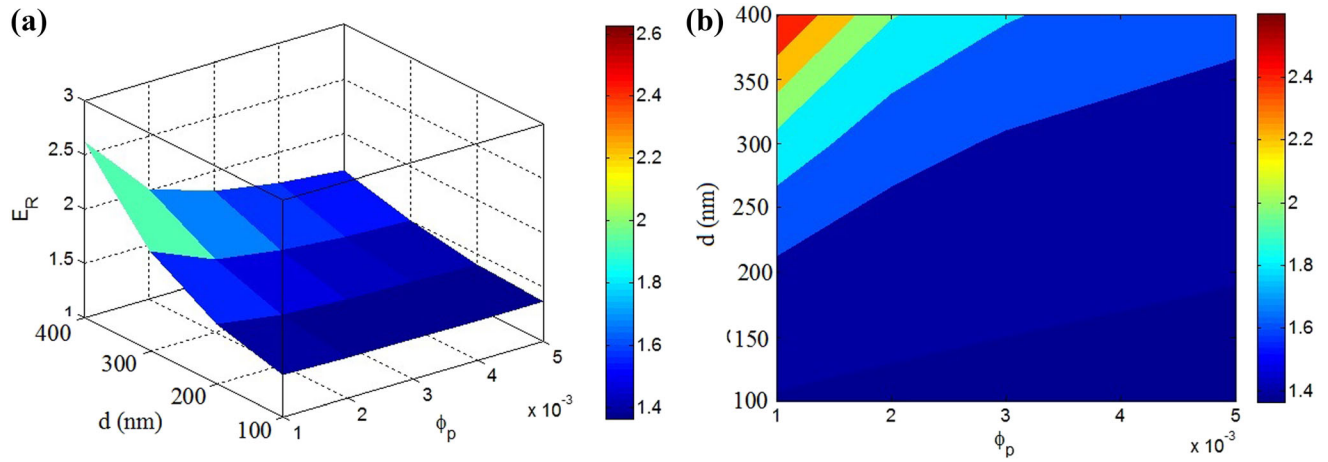

Fig. 5. (a) 3D and (b) contour plots to show the relative modulus at various ϕ_p and d ranges at E_m = 2 GPa, ϕ_f = 0.02, n = 1, and E_f = 1000 GPa.

CONCLUSION

The Paul model was advanced to calculate the tensile modulus of CNT-reinforced nanocomposites by network density depending on filler aspect ratio, percolation onset, CNT diameter, and CNT density. The original and developed models were evaluated by experimental measurements of many examples and the roles of factors in the relative modulus. The experimental results support the accuracy of the advanced model for the samples containing filler networks. However, an undesirable output was reported for the samples with low experimental modulus due to the nonappearance of filler net (below percolation level). Therefore, the advanced model can successfully predict the modulus and network creation in nanocomposites. The highest and the lowest moduli are obtained by the highest and the lowest levels of x, demonstrating the main role of network density in the modulus. This is expected, because a dense network produces a stiff sample that can tolerate a large amount of force. Also, both α and n directly manipulate the relative modulus above percolation onset. A high α shows the high level of interfacial area, which increases the physical involvement of polymer chains with CNT. Likewise, the high quantity of CNT in the network clearly reinforces the samples. A high relative modulus is achieved by low ϕ_p, because ϕ_p determines the minimum filler content creating the network in the polymer medium. Furthermore, high CNT diameter causes a dense network, increasing the modulus of nanocomposites.

ACKNOWLEDGMENTS

This work was supported by the Basic Science Research Program through the National Research Foundation of Korea (NRF) funded by the Ministry of Education, Science, and Technology (Project Number: 2020R1A2B5B02002203).

CONFLICT OF INTEREST

The authors declare that they have no conflict of interest.

REFERENCES

1. S. Chen, M. Sarafbidabad, Y. Zare, and K.Y. Rhee, *RSC Adv.* 8, 23825 (2018).
2. Y. Zare and K.Y. Rhee, *Polymers* 12, 182 (2020).
3. B.G. Compton, N.S. Hmeidat, R.C. Pack, M.F. Heres, and J.R. Sangoro, *JOM* 70, 292 (2018).
4. K. Tserpes, A. Chanteli, and I. Floros, *Compos. Struct.* 168, 657 (2017).
5. A. Naqi, N. Abbas, N. Zahra, A. Hussain, and S.Q. Shabbir, *J. Mater. Res. Technol.* 8, 1203 (2019).
6. A.K. Kasar, G. Xiong, and P.L. Menezes, *JOM* 70, 829 (2018).
7. M.H. Al-Saleh, H.K. Al-Anid, Y.A. Husain, H.M. El-Ghanem, and S.A. Jawad, *J. Phys. D Appl. Phys.* 46, 385305 (2013).
8. M.A. Matos, V.L. Tagarielli, P.M. Baiz-Villafranca, and S.T. Pinho, *J. Mech. Phys. Solids* 114, 84 (2018).
9. S.M. Naghib, Y. Zare, and K.Y. Rhee, *Nanotechnol. Rev.* 9, 53 (2020).
10. A.H.Z. Kalkhoran, S.M. Naghib, O. Vahidi, and M. Rahmanian, *Biomed. Phys. Eng. Express* 4, 055017 (2018).
11. R. Salahandish, A. Ghaffarinejad, E. Omidinia, H. Zargartalebi, K. Majidzadeh-A, S.M. Naghib, and A. Sanati-Nezhad, *Biosens. Bioelectron.* 120, 129 (2018).
12. A. Rostami and M.I. Moosavi, *J. Appl. Polym. Sci.* 137, 48520 (2019).
13. Y. Zare and K.Y. Rhee, *J. Mech. Behav. Biomed. Mater.* 96, 136 (2019).
14. E. Wang, M.S. Tehrani, Y. Zare, and K.Y. Rhee, *Colloids Surf., A* 550, 20 (2018).
15. Y. Zare and K.Y. Rhee, *JOM* 71, 3980 (2019).
16. S. Arora, M. Rekha, A. Gupta, and C. Srivastava, *JOM* 6, 1 (2018).
17. A. Adegbenjo, P. Olubambi, J. Westraadt, M. Lesufi, and M. Mphahlele, *JOM* 71, 2262 (2019).
18. A.M. Okoro, S.S. Lephuthing, S.R. Oke, O.E. Falodun, M.A. Awotunde, and P.A. Olubambi, *JOM* 71, 567 (2019).
19. P.S. Bharadiya, M.K. Singh, and S. Mishra, *JOM* 71, 838 (2019).
20. P. Mishra, B.R. Bhat, B. Bhattacharya, and R. Mehra, *JOM* 70, 1302 (2018).
21. J. Brown, T. Hajilounezhad, N.T. Dee, S. Kim, A.J. Hart, and M.R. Maschmann, *ACS Appl. Mater. Interfaces* 11, 35221 (2019).

22. T. Hajilounezhad, D.M. Ajiboye, and M.R. Maschmann, *Materialia* 7, 100371 (2019).
23. S. Gooneh-Farahani, S.M. Naghib, and M.R. Naimi-Jamal, *Multidiscip. Cancer Investig.* 3, 5 (2019).
24. S. Gooneh-Farahani, M.R. Naimi-Jamal, and S.M. Naghib, *Expert Opin. Drug Deliv.* 16, 79 (2019).
25. Z. Jiao, B. Zhang, C. Li, W. Kuang, J. Zhang, Y. Xiong, S. Tan, X. Cai, and L. Huang, *Nanotechnol. Rev.* 7, 291 (2018).
26. S. Das, C.K. Ghosh, C.K. Sarkar, and S. Roy, *Nanotechnol. Rev.* 7, 497 (2018).
27. W. Chen, G. Lv, W. Hu, D. Li, S. Chen, and Z. Dai, *Nanotechnol. Rev.* 7, 157 (2018).
28. K.R. Mamaghani, S.M. Naghib, A. Zahedi, M. Rahmanian, and M. Mozafari, *Mater. Today Proc.* 5, 15790 (2018).
29. Y. Zare and K.Y. Rhee, *JOM* 71, 3989 (2019).
30. R.M. Boumbimba, K. Wang, N. Bahlouli, S. Ahzi, Y. Rémond, and F. Addiego, *Mech. Mater.* 52, 58 (2012).
31. D. Cai and M. Song, *Compos. Sci. Technol.* 103, 44 (2014).
32. Y. Zare and K.Y. Rhee, *J. Phys. Chem. Solids* 131, 15 (2019).
33. Y. Zare, K.Y. Rhee, and S.J. Park, *J. Biomed. Mater. Res. Part A* 107, 2706 (2019).
34. Y. Zare, H. Garmabi, and K.Y. Rhee, *Sens. Actuators A: Phys.* 295, 113 (2019).
35. A. Farahi, G.D. Najafpour, and A. Ghoreyshi, *JOM* 71, 285 (2019).
36. Y. Zare and K.Y. Rhee, *Polym. Compos.* 161, 601 (2019).
37. Y. Zare, H. Garmabi, and K.Y. Rhee, *Mater. Chem. Phys.* 206, 243 (2018).
38. Y. Zare and K.Y. Rhee, *Polymers* 12, 114 (2020).
39. S. Maiti, S. Suin, N.K. Shrivastava, and B. Khatua, *J. Appl. Polym. Sci.* 130, 543 (2013).
40. E. Garboczi, K. Snyder, J. Douglas, and M. Thorpe, *Phys. Rev. E* 52, 819 (1995).
41. R. Goyal, S. Samant, A. Thakar, and A. Kadam, *J. Phys. D Appl. Phys.* 43, 365404 (2010).
42. Y. Zare and K.Y. Rhee, *J. Mater. Res. Technol.* 9, 22 (2019).
43. N. Jamalzadeh, S. Heidary, Y. Zare, and K.Y. Rhee, *Polym. Test.* 69, 1 (2018).
44. L. Flandin, J. Cavaillé, G. Bidan, and Y. Brechet, *Polym. Compos.* 21, 165 (2000).
45. Y. Zare and K.Y. Rhee, *Compos. Part B: Eng.* 155, 11 (2018).
46. N. Ouali, J. Cavaillé, and J. Perez, *Plast. Rubber Compos. Process. Appl.* 16, 55 (1991).
47. J. Lyngaae-Jorgensen, A. Kuta, K. Sondergaard, and K.V. Poulsen, *Polym. Netw. Blends* 3, 1 (1993).
48. C.J. Plummer, M. Rodlert, J.-L. Bucaille, H.J. Grünbauer, and J.-A.E. Månson, *Polymer* 46, 6543 (2005).
49. Y. Chen, F. Pan, Z. Guo, B. Liu, and J. Zhang, *J. Mech. Phys. Solids* 84, 395 (2015).
50. Z. Zhou, M. Sarafbidabad, Y. Zare, and K.Y. Rhee, *J. Mech. Behav. Biomed. Mater.* 86, 368 (2018).
51. Y. Zare and K.Y. Rhee, *Polymers* 12, 896 (2020).
52. B. Paul. Prediction of elastic constants of multi-phase materials. DTIC Document (1959).
53. Y. Zare and H. Garmabi, *J. Appl. Polym. Sci.* 123, 2309 (2012).
54. N.-H. Tai, M.-K. Yeh, and T.-H. Peng, *Compos. B Eng.* 39, 926 (2008).
55. K. Saeed and S.Y. Park, *J. Appl. Polym. Sci.* 106, 3729 (2007).
56. Q. Zhang, S. Rastogi, D. Chen, D. Lippits, and P.J. Lemstra, *Carbon* 44, 778 (2006).
57. K. Prashantha, J. Soulestin, M. Lacrampe, P. Krawczak, G. Dupin, and M. Claes, *Compos. Sci. Technol.* 69, 1756 (2009).
58. M.A. Bhuiyan, R.V. Pucha, M. Karevan, and K. Kalaitzidou, *Comput. Mater. Sci.* 50, 2347 (2011).
59. A. Szymczyk, Z. Roslaniec, M. Zenker, M.C. García-Gutiérrez, J.J. Hernández, D.R. Rueda, A. Nogales, and T.A. Ezquerra Sanz, *eXPRESS Polym. Lett.* 5, 977 (2011).
60. W. Peng, S. Rhim, Y. Zare, and K.Y. Rhee, *Polym. Compos.* 40, 1117 (2019).
61. A. Khan, M.H. Shamsi, and T.-S. Choi, *Comput. Mater. Sci.* 45, 257 (2009).
62. T. Nazari and H. Garmabi, *Polym. Compos.* 33, 1893 (2012).
63. Y. Zare and K.Y. Rhee, *J. Mater. Res. Technol.* 9, 22 (2020).
64. Y. Zare and K.Y. Rhee, *JOM* 69, 2762 (2017).